6, 25 pg/ml (case 39);day 7, 35 pg/ml (case 36);day 12, 176 pg/ml (case 37) and 1.659 pg/ml (case 34);day 21, 3.700 pg/ml (case 33);day 24, 24 pg/ml (case 38). Thus, the IL-17A production by skin-infiltrating cells were increased and peaked by day 21 and declined thereafter. Considering the time lag of IL-17A production peak between the skin-infiltrating and peripheral blood T cells (see Fig. 1a), it seems that peripheral blood Th17 cells migrate into the skin on day 12–21 after the onset.

In the present study, the percentages of circulating Th17 cells were increased markedly in DIHS and SJS/TEN, and moderately in EM, which is consistent with the previous observation in SJS/TEN [9]. In the clinical course of DIHS, while the frequencies of Th17 and Th2 cells were increased at the early stage and decreased thereafter, activated $CD8^+$ T cells expanded during 2 to 6 weeks after the onset [4] and thus preceded by Th17 and Th2 cells. Th2 cells can respond to causative drugs, and Tc1 cells may be reactive with the virus-infected cells. Plasmacytoid dendritic cells, which have a protective role for viruses, are also decreased at the early stage of DIHS and increased on recovery [10].

Our study demonstrated that Th17 cells are present in the lesional skin as well as the peripheral blood. Compared with the circulating Th17 cells, the appearance of skin-infiltrating Th17 cells seemed to be delayed. It is considered that Th17 cells first expand in the blood and subsequently emigrate into the skin.

Funding source

None.

Acknowledgement

This study was supported by Grants-in-Aid for Scientific Research from the Ministry of Health, Labour, and Welfare in Japan.

References

[1] Hashizume H, Takigawa M, Tokura Y. Characterization of drug-specific T cells in phenobarbital-induced eruption. J Immunol 2002;168:5359–68.
[2] Abe R. Toxic epidermal necrolysis and Stevens–Johnson syndrome: soluble Fas ligand involvement in the pathomechanisms of these diseases. J Dermatol Sci 2008;52:151–9.
[3] Shiohara T, Kano Y, Takahashi R, Ishida T, Mizukawa Y. Drug-induced hypersensitivity syndrome: recent advances in the diagnosis, pathogenesis and management. Chem Immunol Allergy 2012;97:122–38.
[4] Nishio D, Izu K, Kabashima K, Tokura Y. T cell populations propagating in the peripheral blood of patients with drug eruptions. J Dermatol Sci 2007;48:25–33.
[5] Koga C, Kabashima K, Shiraishi N, Kobayashi M, Tokura Y. Possible pathogenic role of Th17 cells for atopic dermatitis. J Invest Dermatol 2008;128:2625–30.
[6] Kabashima R, Sugita K, Sawada Y, Hino R, Nakamura M, Tokura Y. Increased circulating Th17 frequencies and serum IL-22 levels in patients with acute generalized exanthematous pustulosis. J Eur Acad Dermatol Venereol 2011;25:485–8.
[7] Auquier-Dunant A, Mockenhaupt M, Naldi L, Correia O, Schroder W, Roujeau JC. Correlations between clinical patterns and causes of erythema multiforme majus, Stevens–Johnson syndrome, and toxic epidermal necrolysis: results of an international prospective study. Arch Dermatol 2002;138:1019–24.
[8] Hashizume H, Hansen A, Poulsen LK, Thomsen AR, Takigawa M, Thestrup-Pedersen K.. In vitro propagation and dynamics of T cells from skin biopsies by methods using interleukins-2 and -4 or anti-CD3/CD28 antibody-coated microbeads. Acta Derm Venereol 2010;90:468–73.
[9] Tearaki Y, Kawabe M, Izaki S. Possible role of TH17 cells in the pathogenesis of Stevens–Johnson syndrome and toxic epidermal necrolysis. J Allergy Clin Immunol 2013;131:907–9.
[10] Sugita K, Tohyama M, Watanabe H, Otsuka A, Nakajima S, Iijima M, et al. Fluctuation of blood and skin plasmacytoid dendritic cells in drug-induced hypersensitivity syndrome. J Allergy Clin Immunol 2010;126:408–10.

Toshiharu Fujiyama[a1], Chika Kawakami[b1], Kazunari Sugita[b], Rieko Kubo-Kabashima[b], Yu Sawada[b], Ryosuke Hino[b], Motonobu Nakamura[b], Takatoshi Shimauchi[a], Taisuke Ito[a], Kenji Kabashima[c], Hideo Hashizume[d], Yoshiki Tokura[a*]
[a]*Department of Dermatology, Hamamatsu University School of Medicine, Hamamatsu, Japan*;
[b]*Department of Dermatology, University of Occupational and Environmental Health, Kitakyushu, Japan*;
[c]*Deparment of Dermatology, Faculty of Medicine, Kyoto University Graduate School of Medicine, Kyoto, Japan*;
[d]*Section of Dermatology, Shimada City Hospital, Shimada, Japan*

[*]Corresponding author at: Department of Dermatology, Hamamatsu University School of Medicine, 1-20-1 Hanadayama, Higashi-ku, Hamamatsu 431-3192, Japan. Tel.: +81 53 435 2303; fax: +81 53 435 2368
E-mail address: tokura@hama-med.ac.jp
(T. Fujiyama)

[1]These authors equally contributed to this study.

Received 22 April 2013

http://dx.doi.org/10.1016/j.jdermsci.2013.08.008

LETTERS TO THE EDITOR

Deep venous thrombosis associated with cytomegalovirus reactivation in drug-induced hypersensitivity syndrome

Editor

Drug-induced hypersensitivity syndrome (DIHS) is a severe drug allergy characterized by damage to multiple extracutaneous organs and frequent reactivation of human herpesviruses (HHVs) during the disease course.[1] This is the first case of simultaneous emergence of deep venous thrombosis (DVT) and CMV reactivation in a DIHS patient.

A 78-year-old male patient with an 8-day history of recurrent fever, general fatigue and nausea was transferred to our hospital. Physical examination revealed fever (38.6°C) and respiratory distress. At the time of admission, the anti-CMV IgG was 6.4 (ELISA, normal, <2), and the anti-CMV IgM was 0.45 (normal, <0.8). Chest roentgenography and computed tomography demonstrated bilateral interstitial shadows in the bilateral lung fields, suggestive of atypical pneumonitis. Minocycline was started. Twenty-two days after admission, AST and ALT suddenly increased to 114 and 139 U/L respectively. Four days later, high fever suddenly developed with simultaneous emergence of facial oedematous erythema and a maculopapular rash (Fig. 1a). A remarkable increase in white blood cells (16 800/μL) was observed with increased neutrophils (15 080/μL), atypical lymphocytosis (2%) and monocytosis (660/μL). Skin biopsy of the abdominal lesion disclosed mild lymphocytic infiltration into the epidermis and adnexal appendages with focal necrotic keratinocytes (Fig. 1b). Based on the criteria of the Japanese consensus group, diagnosis of 'possible' DIHS was made.[1] Thus, minocycline was discontinued. Administration of prednisolone at 50 mg/day relieved skin manifestations; the prednisolone was gradually reduced to 10 mg/day for 3 weeks thereafter without recurrence. On the sixth day of administration of prednisolone 10 mg/day, his lower legs swelled acutely, and erythematous macules developed again over the trunk and extremities with severe facial oedema and high fever (>38.8°C), suggestive of a flare up of symptoms in DIHS.[1] Laboratory data revealed a high C-reactive protein level (7.93 mg/dL) and increased AST and ALT levels (44 and 59 U/L respectively). In addition to these findings, we observed increased levels of D-dimers (7.3 μg/mL; normal, <1 μg/dL). Neither anti-cardiolipin antibody nor lupus anticoagulant was detected. Computed tomography revealed a large thrombosis from the inferior caval vein to bilateral iliac veins and popliteal veins (Fig. 1c and 1d) as a concomitant medical problem. At that time, we detected seroconversion of CMV IgG and IgM (52.6 and 3.68 respectively), although no cells positive for CMV antigen pp65 was observed. Anticoagulant therapy with heparin was initiated while continuing prednisolone at

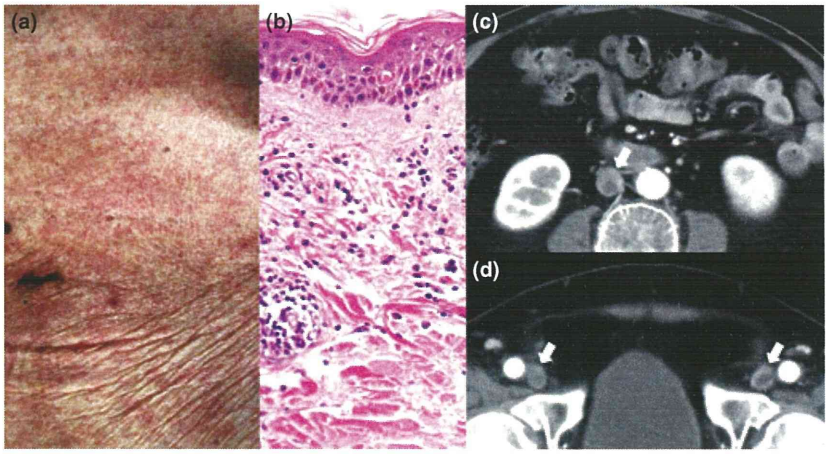

Figure 1 Clinical and pathological features of the present case. Skin biopsy of the maculopapular rash spreading on the abdominal skin (a) reveals lymphocytic infiltration into the epidermis and appendages of the skin (b) (HE staining, original ×400). During the course, thromboses were found in the inferior caval vein (c) and bilateral femoral veins (d). Arrows indicate thrombosed veins on contrast-enhanced computed tomography images.

10 mg/day. AST and ALT gradually returned to normal levels in 2 weeks. The rash disappeared with resolution of leg swelling without medication for CMV infection.

We found that CMV seroconversion was chronologically associated with development of DVT in this case. In spite of accumulating cases of DIHS with CMV reactivation and its complications,[2–5] there has been no case of DVT during DIHS, suggesting that it might have been underestimated. The presence of risk factors plays a prominent role in assessing the pretest probability of DVT: acute infection, older age (>75 years), burden cancers and previous history of thrombosis.[6] In this case, although the patient was aged, no previous history of burden cancers or thrombosis enhanced a crucial contribution of CMV to development of DVT. Two recent case–control studies proved that CMV infection was independently associated with thrombosis among a whole cohort.[7,8] This may occur because of the effect of a procoagulant on endothelial cells[9] or induction of anti-phospholipid antibody that binds to the molecules, mimicking CMV antigens.[10]

We should draw attention to development of DVT as a serious complication of DIHS in addition to well-known serious sequels by CMV reactivation, such as encephalitis, carditis, gastroenteritis and pneumonia.

Acknowledgements

This study was supported in part by a Grant-in-Aid for Scientific Research (No. 21591458) and a Health and Labor Sciences Research Grant (Research on Intractable Diseases) from the Ministry of Health, Labour and Welfare of Japan (H23-nanchi-ippan-003).

H. Hashizume,* M. Hata
Department of Dermatology, Shimada Municipal Hospital, 1200-5 Noda, Shimada, 427-8502 Japan
*Correspondence: H. Hashizume. E-mail: hihashiz0001@mac.com

References

1 Shiohara T, Inaoka M, Kano Y. Drug-induced hypersensitivity syndrome (DIHS): a reaction induced by a complex interplay among herpesviruses and antiviral and antidrug immune responses. *Allergol Int* 2006; **55**: 1–8.
2 Hashizume H, Takigawa M. Drug-induced hypersensitivity syndrome associated with cytomegalovirus reactivation: immunological characterization of pathogenic T cells. *Acta Derm Venereol* 2005; **85**: 47–50.
3 Sano S, Ueno H, Yamagami K *et al.* Isolated ileal perforation due to cytomegalovirus reactivation during management of terbinafine hypersensitivity. *World J Gastroenterol* 2010; **16**: 3339–3342.
4 Asano Y, Kagawa H, Kano Y, Shiohara T. Cytomegalovirus disease during severe drug eruptions: report of 2 cases and retrospective study of 18 patients with drug-induced hypersensitivity syndrome. *Arch Dermatol* 2009; **145**: 1030–1036.
5 Seishima M, Yamanaka S, Fujisawa T, Tohyama M, Hashimoto K. Reactivation of human herpesvirus (HHV) family members other than HHV-6 in drug-induced hypersensitivity syndrome. *Br J Dermatol* 2006; **155**: 344–349.
6 Alikhan R, Cohen AT, Combe S *et al.* Risk factors for venous thromboembolism in hospitalized patients with acute medical illness: analysis of the MEDENOX Study. *Arch Intern Med* 2004; **164**: 963–968.
7 Tichelaar VY, Sprenger HG, Makelburg AB, Niesters BG, Kluin-Nelemans HC, Lijfering WM. Active cytomegalovirus infection in patients with acute venous thrombosis: a case–control study. *Am J Hematol* 2011; **86**: 510–512.
8 Atzmony L, Halutz O, Avidor B *et al.* Incidence of cytomegalovirus-associated thrombosis and its risk factors: a case-control study. *Thromb Res* 2010; **126**: e439–e443.
9 Squizzato A, Gerdes VE, Buller HR. Effects of human cytomegalovirus infection on the coagulation system. *Thromb Haemost* 2005; **93**: 403–410.
10 Gharavi AE, Pierangeli SS, Espinola RG, Liu X, Colden-Stanfield M, Harris EN. Antiphospholipid antibodies induced in mice by immunization with a cytomegalovirus-derived peptide cause thrombosis and activation of endothelial cells *in vivo*. *Arthritis Rheum* 2002; **46**: 545–552.

DOI: 10.1111/j.1468-3083.2012.04560.x

Umbilical cord mesenchymal stem cell transplantation in drug-induced Stevens-Johnson syndrome

Editor

Stevens-Johnson syndrome (SJS) is an acute skin and mucosal membranes inflammatory disease.[1] This disease is rare with annual incidence of 1.2–6.0 per million persons, but serious and potentially life-threatening. Case reports have shown benefit with the use of immunosuppressive agents, plasmapheresis, systemic corticosteroids, intravenous immunoglobubin and TNF-α inhibitors.[2,3] However, the treatment with systemic corticosteroids and other immunosuppressive agents is controversial because of a possible increased risk of sepsis.[4]

Mesenchymal stem cells (MSCs) are a heterogeneous subset of stromal stem cells with the capacity for self-renewal, multipotent differentiation and immunomodulation. Recent research studies have demonstrated the ability of MSC homing to injured tissues and its contribution to tissue repair or regeneration.[5] Culture expanded MSCs could promote the healing of diabetic wounds, [6] implying a profound therapeutic potential for skin wounds and burns. In this study, we will investigate the effect of umbilical cord MSC (UC-MSC) on severe cutaneous lesion in SJS patients.

From August 2009 to March 2011, three female SJS patients ranging in age from 42 to 62 years were enrolled in a MSC transplantation (MSCT) trial. The trial was conducted in compliance with current Good Clinical Practice standards and in accordance with the principles set forth under the Declaration of Helsinki (1989). The study was approved by the Ethics Committee at The Drum Tower Hospital of Nanjing University Medical School and

Allergy EUROPEAN JOURNAL OF ALLERGY AND CLINICAL IMMUNOLOGY

EAACI

Allergy

ORIGINAL ARTICLE SKIN AND EYE DISEASES

Skin recruitment of monomyeloid precursors involves human herpesvirus-6 reactivation in drug allergy

H. Hashizume[1,2], T. Fujiyama[1], J. Kanebayashi[1], Y. Kito[1], M. Hata[1] & H. Yagi[1]

[1]Department of Dermatology, Hamamatsu University School of Medicine, Hamamatsu; [2]Department of Dermatology, Shimada Municipal Hospital, Shimada, Japan

To cite this article: Hashizume H, Fujiyama T, Kanebayashi J, Kito Y, Hata M, Yagi H. Skin recruitment of monomyeloid precursors involves human herpesvirus-6 reactivation in drug allergy. *Allergy* 2013; **68**: 681–699.

Keywords
$CD4^+$ T lymphocyte; drug-induced hypersensitivity syndrome; high-mobility group box-1; human herpesvirus-6, monocyte.

Correspondence
Hideo Hashizume, MD, PhD, Department of Dermatology, Shimada Municipal Hospital, 1200-5 Noda, Shimada, Shizuoka 427-8502, Japan.
Tel.: +81-547-35-2111
Fax: +81-547-36-9511
E-mail: hihashiz0001@mac.com

Accepted for publication 27 January 2013

DOI:10.1111/all.12138

Edited by: Thomas Bieber

Abstract

Background: In drug-induced hypersensitivity syndrome (DIHS), latent human herpesvirus (HHV)-6 is frequently reactivated in association with flaring of symptoms such as fever and hepatitis. We recently demonstrated an emergence of monomyeloid precursors expressing HHV-6 antigen in the circulation during this clinical course.

Methods: To clarify the mechanism of HHV-6 reactivation, we immunologically investigated peripheral blood mononuclear cells (PBMCs), skin-infiltrating cells, and lymphocytes expanded from skin lesions of patients with DIHS.

Results: The circulating monomyeloid precursors in the patients with DIHS were mostly $CD11b^+CD13^+CD14^-CD16^{high}$ and showed substantial expression of skin-associated molecules, such as CCR4. $CD13^+CD14^-$ cells were also found in the DIHS skin lesions, suggesting skin recruitment of this cell population. We detected high levels of high-mobility group box (HMGB)-1 in blood and skin lesions in the active phase of patients with DIHS and showed that recombinant HMGB-1 had functional chemoattractant activity for monocytes/monomyeloid precursors *in vitro*. HHV-6 infection of the skin-resident $CD4^+$ T cells was confirmed by the presence of its genome and antigen. This infection was likely to be mediated by monomyeloid precursors recruited to the skin, because normal $CD4^+$ T cells gained HHV-6 antigen after *in vitro* coculture with highly virus-loaded monomyeloid precursors from the patients.

Conclusions: Our results suggest that monomyeloid precursors harboring HHV-6 are navigated by HMGB-1 released from damaged skin and probably cause HHV-6 transmission to skin-infiltrating $CD4^+$ T cells, which is an indispensable event for HHV-6 replication. These findings implicate the skin as a cryptic and primary site for initiating HHV-6 reactivation.

Latent human herpesvirus (HHV)-6 is occasionally reactivated to manifest itself as virus-associated diseases that jeopardize the hosts. Drug-induced hypersensitivity syndrome (DIHS), also known as drug rash with eosinophilia and systemic symptoms, is a distinct entity of severe drug hypersensitivity because of its characteristic features (1, 2). HHV-6 reactivation has been found in more than 60% of such cases in association with unfavorable outcomes (3, 4), but the mechanisms remain unknown. To clarify this issue, we immunologically investigated peripheral and skin-infiltrating cells in DIHS. Our results suggest that skin recruitment of monomyeloid precursors navigated by high-mobility group box (HMGB)-1 is a crucial event in HHV-6 reactivation in DIHS.

Materials and methods

Patients

Twenty-seven patients with DIHS were enrolled in this study (Table 1). In addition, three normal male individuals and 24 patients with other types of drug eruptions (Stevens–Johnson syndrome (SJS), 9; toxic epidermal necrolysis (TEN), 3; maculopapular eruption (MPE), 8; and acute generalized

Table 1 DIHS patient profiles

Patient	Age/Gender	Culprit drug	Virus reactivation*
1	47/M	CBZ	HHV-6/CMV
2	49/M	CBZ	HHV-6
3	25/F	CBZ	HHV-6/HHV-7/CMV
4	73/F	CBZ	HHV-6/EBV/CMV
5	72/F	CBZ	HHV-6
6	51/M	CBZ	HHV-6/HHV-7
7	25/M	CBZ	HHV-7
8	89/F	CBZ	N.D.
9	42/F	CBZ/Phenytoin	HHV-6
10	68/M	Allopurinol	HHV-6
11	82/M	Allopurinol	HHV-7/EBV
12	54/M	Allopurinol	CMV
13	86/M	Allopurinol	HHV-6/CMV
14	53/F	Salazosulfapyridine	N.D.
15	46/F	Salazosulfapyridine	HHV-6
16	33/F	Salazosulfapyridine	HHV-6
17	48/F	Mexiletine	HHV-6/HHV-7
18	82/M	Mexiletine	HHV-7
19	57/F	Phenobarbital	HHV-6/CMV
20	60/M	Phenobarbital	HHV-6/CMV
21	43/F	Phenobarbital	HHV-6
22	42/M	Tribenoside	CMV
23	55/F	Tribenoside	HHV-6/CMV
24	18/F	Zonisamide	HHV-6/HHV-7
25	63/F	Zonisamide	HHV-6
26	40/M	Phenytoin	N.D.
27	69/F	Minocyclin	CMV

CBZ, carbamazepine, HHV, human herpesvirus; CMV, cytomegalovirus; EBV, Epstein–Barr virus; N.D., no data.
*Antibodies against viruses that increased in titer in paired serum samples are indicated.

exanthematous pustulosis (AGEP), 4) were investigated. The study was performed according to the Declaration of Helsinki, and the study protocol was approved by the Hamamatsu University School of Medicine Ethical Committee. Written informed consent was obtained from all participants.

Reagents, monoclonal antibodies (mAbs), and culture medium

FITC-conjugated, PE-conjugated, and PerCP-conjugated mAbs against CD3, CD4, CD8, CD16, CD45, cutaneous lymphocyte antigen (CLA), HLA-DR, CD11b, CD13, CD14, CD34, CD117, and CD163 were purchased from BD PharMingen (San Diego, CA, USA). mAbs against CCR1 to CCR10 and CXCR1 to CXCR6 were obtained from R&D Systems (Minneapolis, MN, USA). A mouse anti-HHV-6 A and B variants mAb (clone 7C7 45/15) was obtained from Argene SA (Varilhes, France). A mouse anti-HMGB-1 mAb (clone J2E1) was obtained from ATGen (Gyeonggi-do, South Korea). Recombinant human HMGB-1 was obtained from R&D Systems Inc. Cells were cultured in RPMI 1640 medium (Life Technologies, Carlsbad, CA, USA) supplemented with L-glutamine, sodium pyruvate, 2-mercaptoethanol, nonessential amino acids (Life Technologies), and 10% heat-inactivated fetal calf serum or pooled human AB serum (cRPMI) as previously described (5). For expansion of T lymphocytes, the medium was supplemented with human recombinant IL-2 (R&D Systems) and/or anti-CD3/CD28 Ab-conjugated microbeads (T-cell Expander; Dynal, Copenhagen, Denmark) as previously reported (5).

Cell preparation

Blood samples were taken from the normal individuals and serially from the patients with DIHS during the disease course and after the resolution in some cases. Peripheral blood mononuclear cells (PBMCs) were isolated from the heparinized whole-blood samples by Ficoll–Hypaque (Pharmacia Fine Chemicals, Uppsala, Sweden) gradient centrifugation. After placement in plastic plates for 1–3 h, the adherent cells were used as a monocyte/monomyeloid precursor-rich fraction. For chemotaxis assay, the cells were recovered by gently scraping with a plastic cell scraper and transferred to a 15-ml conical tube to centrifuge 10 min at 300 ***g*** and thus were transferred to new plates, maintained in culture with cRPMI containing GM-CSF at 10 ng/ml as a survival factor for prolonged explanted culture (6). CD4+ T cells were isolated from PBMCs with a CD4+ T-cell isolation kit (Miltenyi Biotec., Gladbach, Germany) according to the manufacturer's protocol. Skin-derived T cells were obtained by culturing skin samples for 72 h and expansion as described previously (5).

PCR for detection of HHVs

DNA was extracted from cultured cells using a DNeasy Kit (Qiagen, Valencia, CA, USA) according to the manufacturer's protocol. For detection of HHVs including Epstein–Barr virus (EBV), HHV-6, HHV-7, and cytomegalovirus (CMV), appropriate DNA samples and positive DNA controls (HHV-6, HHV-7, and EBV) were amplified by multiplex nested PCR with specific primers as described previously (7). After amplification of specific virus gene fragments, the products were electrophoresed in a 4% agarose gel, stained with ethidium bromide, and visualized under ultraviolet light.

Flow cytometry

Aliquots containing 1×10^4 PBMCs were stained with fluorescence-conjugated mAbs against the target molecules and analyzed as described previously (8). HHV-6 antigen (Ag) detection was performed with an anti-HHV-6 Ab using a similar method to that described for intracytoplasmic cytokine staining (8).

Real-time horizontal chemotaxis assay

An optically accessible horizontal chemotaxis apparatus (EZ-TAXIScan; GE Healthcare UK Ltd., Buckinghamshire, UK) was used to evaluate the chemotactic activity of the cells, as previously described (9). The apparatus consisted of

front and back chambers containing cells and a chemoattractant, respectively, which were connected by a microchannel. Cells present within the microchannel (50 μm in length) during observation periods were successively recorded at 30-s intervals on a computer equipped with a video camera. Data were analyzed using the Image J software (National Institutes of Health, Bethesda, MD, USA) and the Manual Tracking plug-in produced by FP Cordelieres (Institut Curie; http://rsbweb.nih.gov/ij/plugins/track/track.html).

Measurement of the plasma HMGB-1 concentration

The plasma HMGB-1 concentrations were measured using an HMGB-1 ELISA Kit (Shino-Test Co., Tokyo, Japan) according to the manufacturer's protocol.

Immunofluorescence staining

After fixation with acetone for 5 min, smear slides of cultured cells and snap-frozen skin sections (5 μm thick) were incubated with fluorochrome-conjugated Abs against the target molecules. Some specimens were incubated with a primary Ab and then incubated with a fluorescently tagged anti-mouse Ig secondary Ab after a blocking procedure. Nuclear counterstaining was performed with DAPI. The specimens were observed under a fluorescence microscope with filters for excitation at 490 and 540 nm. Specimens with omission of the primary Abs served as controls.

Electron microscopy

Samples were fixed with 2% paraformaldehyde and 2.5% glutaraldehyde in 0.1 M cacodylate buffer, postfixed with OsO_4, and stained with uranyl acetate. After embedding in epoxy resin, ultrathin sections were examined under an electron microscope (JEM1220; Jeol Datum Ltd., Tokyo, Japan) and recorded with a CCD camera.

Statistical analysis

Pair-matched differences were analyzed by the Wilcoxon signed rank test, and comparisons among multiple samples were analyzed by Dunn's multiple comparison test and the Mann–Whitney U-test using the software GraphPad Prism 5 (GraphPad Software Inc., La Jolla, CA, USA). Values of $P < 0.05$ were considered to indicate statistical significance.

Results

Circulating HHV-6-positive monomyeloid precursors are recruited to the skin lesions of DIHS

We previously found a novel fraction (R1), which were distinct from a monocyte population (R2), in circulation during the course of DIHS (Fig. 1A) (10). The percentage of this fraction (R1) was increased in the early phase (<21 days after onset; mean ± SD, 9.9 ± 5.1%) and then returned to a normal level in the late phase (≥21 days after onset; 2.5 ± 1.1%) ($P = 0.0039$, Wilcoxon signed rank test). These cells were exclusively $CD13^+$ and $CD11b^+$ and largely $CD14^-$ (Fig. 1A, Fig. S1). They also variably, but substantially, expressed CD16, CCR4, CCR7, CXCR4, and CLA (Fig. 1A), with no or marginal expression of CCR1, 2, 3, 5, 6, 8, and 9 and CXCR1, 2, 3, and 5 (data not shown). A minor subset (~15%) of these cells also expressed CCR10. A macrophage marker, CD163, and stem cell markers, such as CD34 and CD117, were hardly detected (Fig. S1). These findings suggest that the cells belong to an immature/precursor type of the monomyeloid lineage in the bone marrow (11), and we designated them as monomyeloid precursors. The subset was marginally detected (<2%) in MPE ($n = 9$), SJS ($n = 8$), and TEN ($n = 3$). In these cells, we detected HHV-6 genome by multiplex nested PCR analysis (Fig. 1B, upper) and virus particles by electron microscopic analysis (Fig. 1C) as well as high expression of HHV-6 Ag by flow cytometric analysis (Fig. 1B, lower, Fig. S2).

Immunofluorescence staining revealed marked $CD13^+$ cells and $CD14^-$ or $CD11b^+$ in the dermis of the early stage of DIHS skin lesions ($n = 4$, Fig. 1D, left), where HHV-6 genome was simultaneously detected by PCR (Fig. 3B, Lane 1). However, lower infiltrates of these cells were observed in the dermis of AGEP skin lesions (Fig. 1D, Fig. S3), MPE, and SJS (data not shown), where HHV-6 genome was hardly detected (Fig. 3B, Lane 4).

HMGB-1 navigates monomyeloid precursors to the skin in DIHS

HMGB-1, a member of the damage-associated molecular pattern molecule (DAMP) family (12–16), may be a candidate for a chemoattractant for the monomyeloid precursors in DIHS. We measured the plasma concentrations of HMGB-1 at various time points in patients with DIHS ($n = 17$) as well as in patients with SJS ($n = 3$) and normal subjects ($n = 3$) (Fig. 2A). The plasma HMGB-1 levels in the early phase of DIHS were significantly higher ($n = 17$; mean ± SD, 8.61 ± 5.5 ng/ml) than those in the late phase ($n = 12$; 4.43 ± 1.45 ng/ml) and were much lower in the normal individuals (2.96 ± 0.53 ng/ml) (Dunn's multiple comparison test, $P < 0.05$ and $P < 0.01$, respectively). It was noted that two patients had extremely high levels of HMGB-1 in the early phase of DIHS (21.2 and 23.0 ng/ml), which were comparable to the levels in patients with sepsis (17). We also observed high levels of HMGB-1 in the patients with SJS (9.01, 6.05, and 6.0 ng/ml), consistent with a previous study (18).

To confirm that HMGB-1 is a functional navigator of the monomyeloid precursors, we performed real-time horizontal chemotaxis assays for the monocyte/monomyeloid precursor-rich fractions from the PBMCs of normal individuals ($n = 3$) and three patients with DIHS (#13, #15, and #16 in Table 1) using a cellular chemotaxis measurement device that offers advantages over existing methods by analyzing small numbers of cells. We observed significant chemotactic activity of recombinant HMGB-1 for healthy monocytes, following a Gaussian curve, with the maximum response at 8–40 ng/ml.

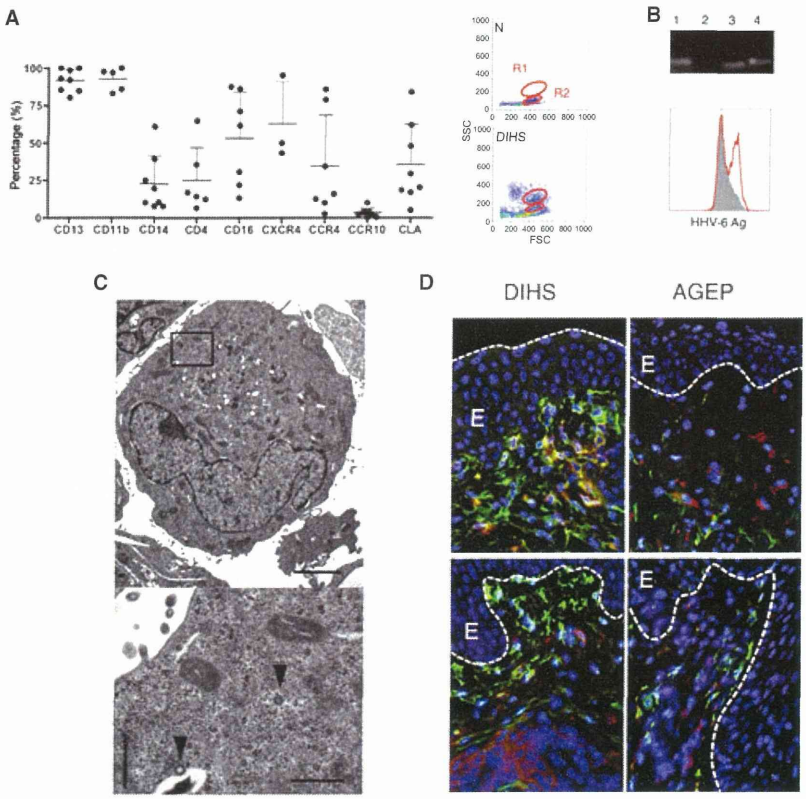

Figure 1 Characterization of circulating monomyeloid precursors. (A) Phenotype of the circulating monomyeloid precursors (R1) in DIHS patients ($n = 17$). These cells are distinct from monocytes (R2) in SSC levels. The percentages of the cells expressing the molecules investigated are indicated. Horizontal bars: mean values; vertical bars with small horizontal bars: standard deviations. N, normal. (B) Detection of HHV-6. Upper: PCR analysis of the HHV-6 genome in the monomyeloid precursor-rich fraction. Multiplex nested PCR for the detection of HHVs was performed. Lane 1, monomyeloid precursors; lane 2, normal PBMCs; lane 3, EBV-infected cells; lane 4, HHV-6 genome. Lower: flow cytometric analysis of HHV-6 Ag in the monomyeloid precursor-rich fraction as purified in the PCR analysis. HHV-6 Ag expression was investigated in patients. Red line, monomyeloid precursors; gray shading: isotype. *X*-axis, HHV-6 Ag; *Y*-axis, cell number. (C) Electron microscopic observation of the monomyeloid precursors. The arrowheads indicate small round structures. Bars = 3 μm (upper) and 0.6 μm (lower). (D) Immunofluorescence staining of skin lesions in DIHS and AGEP. Double immunofluorescence staining was performed with FITC-anti-CD13 and PE-anti-CD14 Abs (lower panels) and with FITC-anti-CD13 and PE-anti-CD11b Abs (upper panels). Blue, DAPI; E, epidermis. Original magnification: ×400.

On the other hand, we found a significant chemotactic response of this molecule for the cells of the monomyeloid precursor-rich fractions only at 40 ng/ml. The effect was significantly abrogated by addition of a neutralizing Ab (Fig. 2B, right).

Next, we performed immunofluorescence staining of HMGB-1 in skin lesions. In normal skin, HMGB-1 was expressed in the nuclei of keratinocytes ($n = 2$, Fig. 2C, a–d), consistent with previous findings (19, 20). In contrast, strong expression of HMGB-1 in the cytoplasm of entire epidermal cells, infiltrating cells, and interstitial tissues of the dermis was found in DIHS lesions while diminished nuclear expression was noted ($n = 3$, Fig. 2C, e–h). These observations suggest that translocation of HMGB-1 has occurred. We observed that $CD13^+$ cells infiltrated adjacent to keratinocytes with strong HMGB-1 expression (Fig. 2C, h), suggesting chemoattraction for the monomyeloid precursors. On the other hand, HMGB-1 expression was observed in an upper layer of the epidermis in SJS skin lesions ($n = 3$, Fig. 2C, i–l), where $CD13^+$ cells showed marginal infiltration (Fig. 2C, l). The HMGB-1 expression area was larger in DIHS lesions than in SJS lesions and normal skin samples with significant differences (Fig. 2D), in accordance with greater relative HMGB-1 mRNA expression in DIHS skin ($n = 3$) than SJS skin ($n = 3$) although it was not statistically significant ($P = 0.1$) (Fig. S4).

HHV-6 is preferentially transmitted to $CD4^+$ T cells by monomyeloid precursors recruited to the skin

HHV-6 replicates exclusively in activated $CD4^+$ T cells and not in $CD8^+$ T cells or monomyeloid cells (21). Because no HHV-6 Ag is detected in circulating $CD4^+$ cells (10), we examined whether skin-resident T cells were infected with

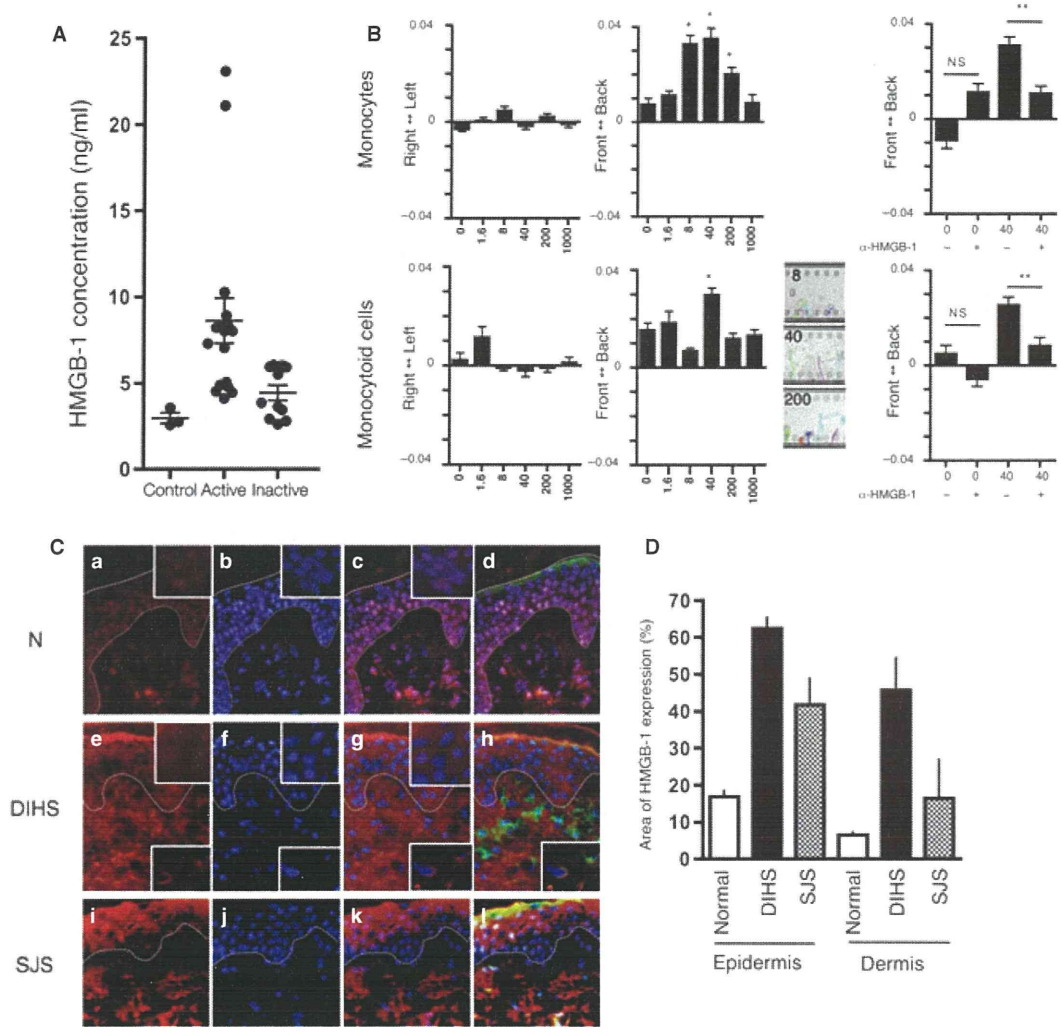

Figure 2 (A) Plasma concentrations of HMGB-1 in patients with DIHS Plasma samples were obtained from normal individuals (controls) and patients with DIHS in the early active (<day 21) and late inactive (≥day 21) phases and measured for their HMGB-1 concentrations (ng/ml) by ELISA. Horizontal bars: mean values; vertical bars with small horizontal bars: standard deviations. $*P < 0.01$, $**P < 0.05$, Dunn's multiple comparison test. (B) Chemotactic activity of HMGB-1 in the cells of the monocyte/monomyeloid precursor-rich fractions. The chemotactic response of the cells from healthy controls (upper) and patients with DIHS (lower) toward HMGB-1 at various concentrations was investigated with an EZ-TAXIScan device. The cell migration velocities in the right–left (left) and front–back (middle, right) directions were calculated and are depicted. The effects of an anti-HMGB-1 Ab on the cell migration are shown in the right panels. The data shown are means ± SD (≥500 cells/case; 3 cases/group are investigated.). The *X*-axis indicates the concentration of HMGB-1 (ng/ml), and the *Y*-axis indicates the velocity of the cell migration (μm/s). The picture panels show traces at around 3000 s in the presence of 8, 40, and 200 ng/ml of HMGB-1. $*P < 0.005$, $**P < 0.001$, Mann–Whitney U-test. (C) HMGB-1 expression in skin. Skin specimens from normal individuals (a–d, $n = 3$), patients with DIHS (e–h, $n = 3$) and patients with SJS (i–j, $n = 2$) were immunostained with an anti-HMGB-1 Ab (red, a, e, j) and anti-CD13 Ab (green, d, h, j). Nuclear staining was performed with DAPI (b, f, j). Representative data are shown. Merged images for HMGB-1/DAPI (c, g, h) and HMGB-1/DAPI/CD13 (d, h, l) are also shown. Original magnification, ×400; Insets, ×1000. Dotted line, epidermal–dermal junction. (D) HMGB-1 expression areas in skin. The data shown are means ± SD (20 areas/case; 3 cases/disease were investigated). The areas were calculated using Image J software. $*P < 0.05$, vs. normal and SJS skin, and $**P < 0.05$, vs. normal skin by the Mann–Whitney U-test.

HHV-6. We expanded skin-resident lymphocytes from three patients with DIHS (#3, #10, and #16 in Table 1) using a previously described method (5). The $CD4^+$ lymphocytes tended to be larger than the $CD8^+$ cells (Fig. 3A), similar to cytopathic lymphocytes after virus infection (22). In fact, HHV-6 Ag (Fig. 3C) and genome (Fig. 3B) were detected exclusively in $CD4^+$, but not in $CD8^+$, cells derived from DIHS skin lesions.

These findings prompted us to investigate whether the monomyeloid precursors harboring HHV-6 transmitted the

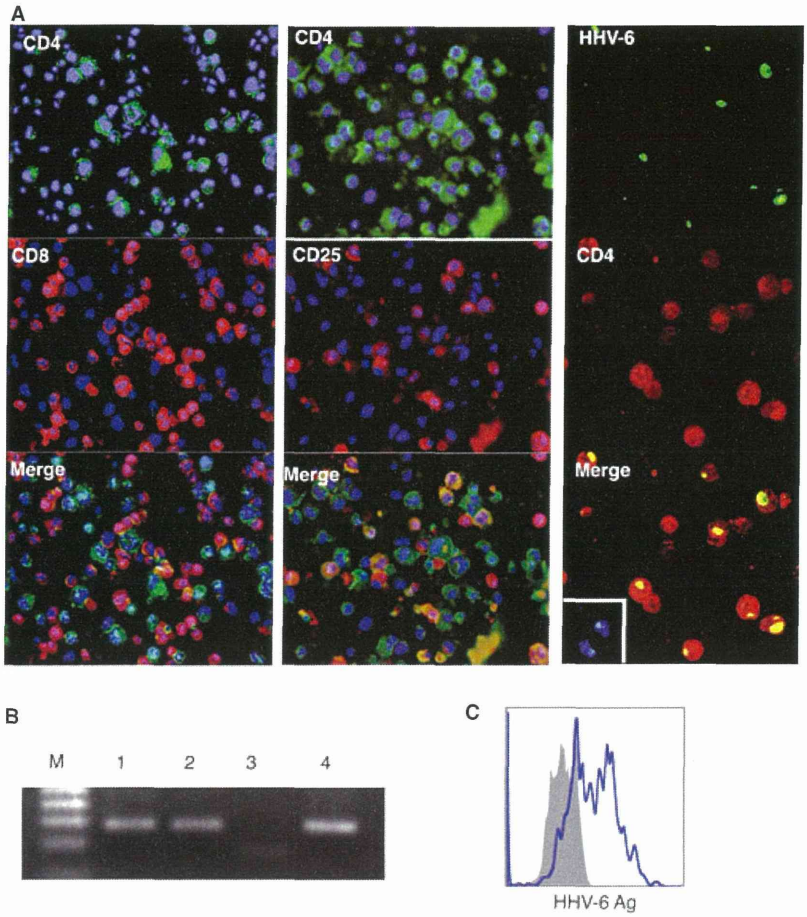

Figure 3 (A) Smear preparation of skin-resident T lymphocytes with immunofluorescence staining for CD4, CD8, CD25, and HHV-6 Ag. Blue, DAPI. Original magnification, ×400. (B) Multiplex nested PCR for detection of HHVs. Lane 1, DIHS skin lesion specimen; lane 2, DIHS skin lesion–resident CD4+ T cells; lane 3, SJS skin lesion–resident T lymphocytes; lane 4, HHV-6 genome as a positive control. (C) HHV-6 Ag expression (blue line) in skin-resident $CD4^+$ T cells. Gray shadow: isotype.

virus to skin-infiltrating $CD4^+$ T cells. We obtained monocytoid cell-rich fractions from cultures of PBMCs from two patients with DIHS (#16 and #19 in Table 1) at two different time points (days 14 and 21). $CD3^+$ T cells isolated from the normal individuals were mixed with each of the cultures containing the monocytoid cell-rich fractions, cultured for 5 days, and then analyzed for HHV-6 Ag by flow cytometry. HHV-6 Ag expression was higher in the 14-day monomyeloid precursor-rich fractions (74.5% and 63.7%) than the day-21 monomyeloid precursor-rich fractions (16.6% and 16.0%) from the two patients (Fig. 4A). After 5 days of coculture of the day-14 monomyeloid precursors and normal lymphocytes, 22% and 18% of the normal $CD4^+$ T cells became positive for HHV-6 Ag in two separate experiments. No HHV-6 Ag was detected in the normal $CD8^+$ T cells (Fig. 4A). On the other hand, HHV-6 Ag was insignificantly (~5%) detected in cocultures with the day-21 monomyeloid precursors. These findings indicate that the monomyeloid precursors preferentially potentiate the transmission of HHV-6 to a $CD4^+$ T-cell subset. Moreover, a high virus load in the monomyeloid precursors is likely to be a prerequisite for HHV-6 transmission.

We performed immunofluorescence staining to detect HHV-6 Ag in skin lesions biopsied at different time points (days 7 and 14 after onset) during the early phase in a patient with DIHS. In the skin lesion at day 7, the majority of cells infiltrating the skin were $CD3^+$ cells, while $CD13^+$ cells were sparsely observed (Fig. 4B, left upper). HHV-6 Ag was slightly detected (Fig. 4B, left lower). However, the skin lesion at day 14 revealed a higher number of infiltrating $CD13^+$ cells with coexpression of HHV-6 Ag as well as $CD3^+$ cells (Fig. 4B, right).

Discussion

Circulating monocytes in normal individuals are divided into two groups: a major $CD14^{high}CD16^-$ 'inflammatory' subset and a minor (<10% of total monocytes) $CD14^{low}CD16^+$ 'resident' subset. The cells in the latter subset differentiate into dendritic cells/macrophages to replenish the tissue-resident

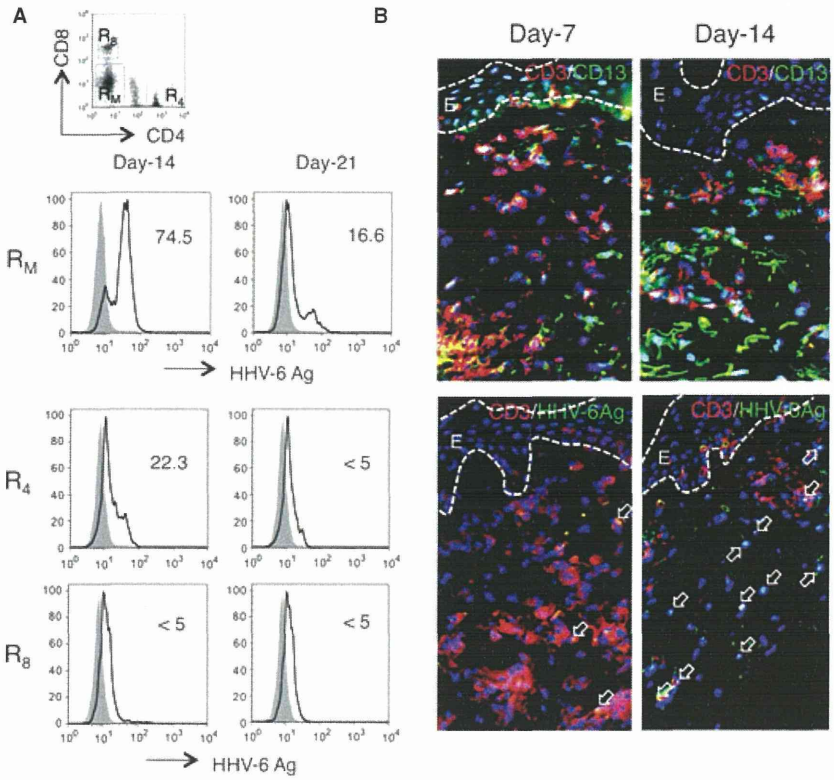

Figure 4 (A) *In vitro* HHV-6 transmission from monomyeloid precursors to allogeneic T lymphocytes. The monocytoid cell-rich fractions (Rm) from a patient with DIHS (#16 in Table 1) at days 14 and day 21 were cocultured with allogeneic T lymphocytes isolated from a healthy individual. After 5 days of culture, HHV-6 Ag expression was analyzed on the basis of the $CD4^+$ fraction (R4) and $CD8^+$ fraction (R8). The numbers indicate the percentages of HHV-6 Ag-positive cells in the total cells. The gray shadows indicate the isotype control. (B) $CD3^+/CD13^+$ cell infiltration and HHV-6 Ag expression in DIHS skin at days 7 and 14. Arrows indicate HHV-6 Ag expression. E, epidermis. Original magnification, ×400.

cells (23–25). On the contrary, the cells of the R1 population in DIHS comprised a minor $CD14^{high}CD16^-$ population and a major $CD14^-$ $CD16^+$ population that expressed skin-associated molecules such as CCR4, CLA markedly, and CCR10 partly, implying that they are precursors of a skin-resident subset. These cells were morphologically and phenotypically similar to monomyeloid precursors in the bone marrow (26), and some of them harbored HHV-6. Because some monomyeloid cells are latently infected with HHV-6 as virus reservoirs (27), the cells in the R1 population appear to have originated from monomyeloid precursors.

DAMPs released from damaged cells are cue signals for initiating immune responses in various organs through their activation after interacting with pattern recognition receptors and/or Toll-like receptors (12–16) and thus promote rapid recruitment of bone marrow-derived leukocytes to the target tissues for inflammation and regeneration in various aseptic inflammatory conditions (28–30), including SJS and TEN (31, 32). HMGB-1, one of the most well-known DAMP members, is a nonhistone protein with dual functions, namely transcriptional regulation by loose binding to chromatin inside cells, and a cue for inflammation outside cells with high potency to attract and activate various immunocompetent cells including monocytes and myeloid cells (12–16, 33). Our study first demonstrated high expression levels of HMGB-1 in blood and skin lesions in DIHS, with chemoattractant potency at 40 ng/ml of recombinant HMGB-1 *in vitro* for the cells of the monomyeloid percursor-rich fraction, suggesting its action as a navigator for skin recruitment of monomyeloid precursors in DIHS. Although a Gaussian curve of the chemotactic response to recombinant HMGB-1, as seen in healthy monocytes, was not found in monomyeloid precursors in DIHS, it might be due to diversity of the cell viability among these patients. Recently, other researchers found high expression levels of HMGB-1 in blood from patients with SJS (18). However, HMGB-1 was expressed at lower levels in SJS lesions than in DIHS lesions, suggesting different roles in each pathogenesis.

It has been demonstrated that a skin rash develops with simultaneous emergence of HHV-6 viremia in severely immunosuppressed patients (31). Therefore, we hypothesize that HHV-6 reactivation primarily starts in the skin of DIHS. Our observations constitute circumstantial evidence for this scenario. Immunohistochemical and immunological experiments proved close contacts of monomyeloid precursors and T cells in the skin and the presence of HHV-6 in skin-resident